

Dedicated to Professor A. Łaszkiewicz in 50th (1926—1976) anniversary  
of his scientific activity

Zofia GUMOWSKA-WDOWIAK \*

**ORIENTED ASSEMBLAGES OF PLAGIOCLASE PHENOCRYSTS  
IN ANDESITES OF THE PIENINY REGION**

UKD 549.651.2:548.57:548.23:552.323.4(438-13 Pieniny)

**A b s t r a c t:** Assemblages consisting of larger plagioclase phenocrysts and orbitally distributed smaller feldspar grains were studied in detail using universal stage method. It was found that these assemblages display twin or nearly twin relations. Moreover, similarly as in glomerophytic aggregations (intergrowths) of plagioclases, they form systems showing higher pseudosymmetry, whereby central grains play the role of ordering element. Calculations based on measurements of the inclination values, sizes and distances of grains within "orbital" system suggest the activity of long range forces in magmatic melt, most probably electrostatic in nature. This activity results in the formation of oriented system studied, representing an intermediate stage of the process of formation of glomerophytic intergrowths.

When examining plagioclase glomerophytic intergrowths (groupings) in andesites of the Pieniny region (Gumowska-Wdowiak, 1974), the present writer observed rather frequent occurrence of characteristic assemblages consisting of larger plagioclase grains surrounded by smaller ones and resembling an orbital system. One of these assemblages, presented in detail in Fig. 1 \*\*, was drawn by means of special apparatus. The distances between the centres of "satellitic" grains and that of the central one (A) were also measured. Crystallographic axes of all the grains in question were determined using universal stage and mutual orientation of twin intergrowths were examined (Tab. 1). It was found that individual crystals — similarly as in twins — are mutually rotated by more or less regular operation of diads which are nearly parallel to crystallographic directions — often less common ones (Fig. 2) \*\*\*. These axes form se-

\* Museum of the Earth, Polish Academy of Sciences, Warsaw, Al. Na Skarbie 20/26.

\*\* Hornblende andesite, Krupianka stream — average composition of plagioclase — 47% An.

\*\*\* More than one symbol a given axis is due to cooperation of twins of the same type (Albite, Pericline or corresponding triadic ones). Symbols with the mark of equality indicate that a given axis is both the edge and the normal of a face. This also refers to ideal projection.

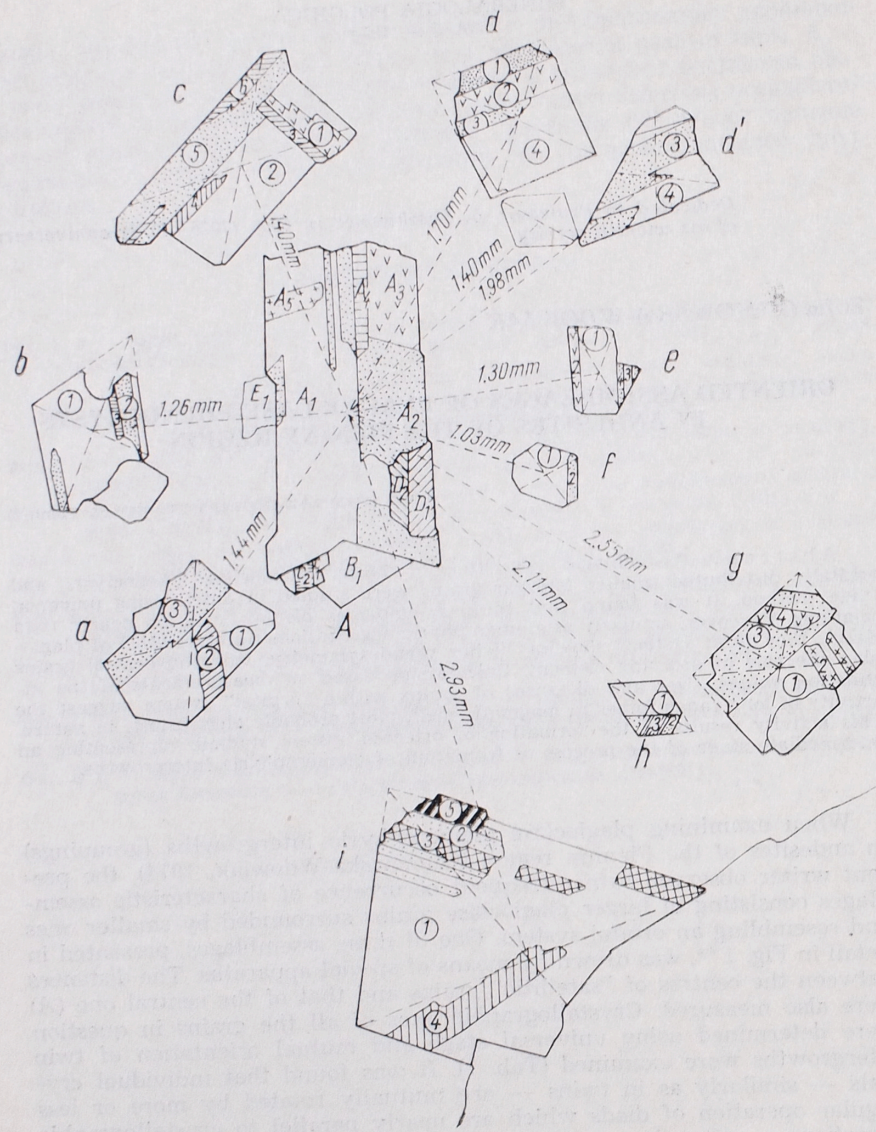


Fig. 1. Oriented assemblage of plagioclase grain in andesite from Krupianka stream, Pieniny Mts.

quences of mutual geometric relations, though do not project precisely on common great circles. This is caused by some deviations from mutually ideal symmetric position of grains.

In order to examine "twin" orientation and other geometric relations of not contacting grains it was necessary to construct such ideal projection

which would contain all the elements of symmetry of the real one. This projection was constructed on the basis of a real sequence of axes denoted by Roman number I (Fig. 2) and satisfying two fundamental conditions. 1) it contains the axes combining 5 grains (A, a, b, d and g) whereby 2) the axes project possibility close to one great circle. In order to present all the relations found in an ideal forms, it was necessary to change the

Table 1

Twinning of individual grains

No.	Grain	[010]	(001)	$\perp [010] / (001)$	(010)	[001]	$\perp [001] / (001)$
1	$A_{12345}$	12,34	13,24	14,23	15		
2	$a_{123}$	12			13		
3	$b_{123}$	12	23	13			
4	$c_{123456}$	12	13	23	24,56	25,46	26,45
5	$d_{1234}$	12,34	13,34	14,23			
6	$e_{1234}$				12,34	14,23	13,24
7	$f_{12}$	12					
8	$g_{1234}$	12,34					13
9	$h_{123}$	12			23		
10	$i_{1234}$	12	13	23	14		

angular distance between initial axes of this sequence, i.e.,  $b(21\bar{1})_{A_1b_2}$  and  $b(12\bar{1})_{A_1a_3}$  ( $b$  — bisectrix) and to accept such great circle, the normal of which ([125] edge) forms an angle of  $55^\circ$  with Y axis of the A grain. These initial data were determined by means of graphical approximation. Three individual axes project distinctly on this circle ( $b_{12}d_{21}$ ,  $a_3d_1$  and  $b_{12}g_{43}$ ) while the remaining three deviate within the limits from  $1$  to  $4^\circ$ .

In an ideal projection (Fig. 3) on a plane perpendicular to Y axis of the A grains, Albite directions of  $a_{13}$ ,  $c_{24}$  and  $g_{13}$  individuals and Pericline ones of  $A_{12,34}$ ,  $h_{12}$  and  $i_{12,3}$  grains, forming the angles of  $88^\circ$ , are overlapping. Two multi-axial sequences (II and IX, Fig. 3) are situated perpendicular to the former ones. Their axes result both from direct "twin" relation between grains in question and from triad intergrowths observed in them. There occur here all the sequences of axes of real projection from I to VIII and further four — from IX to XII, resulting from ideal projection. The change of indices of some axes is also due to this projection.

When considering individual sequences from point of view of geometric transformations, we find at least 4 axes forming a closed transformation cycle, allowing to go back to the initial position. Let us present a transformation scheme "p" exemplified by 4 axes of the sequence I (Fig. 1).

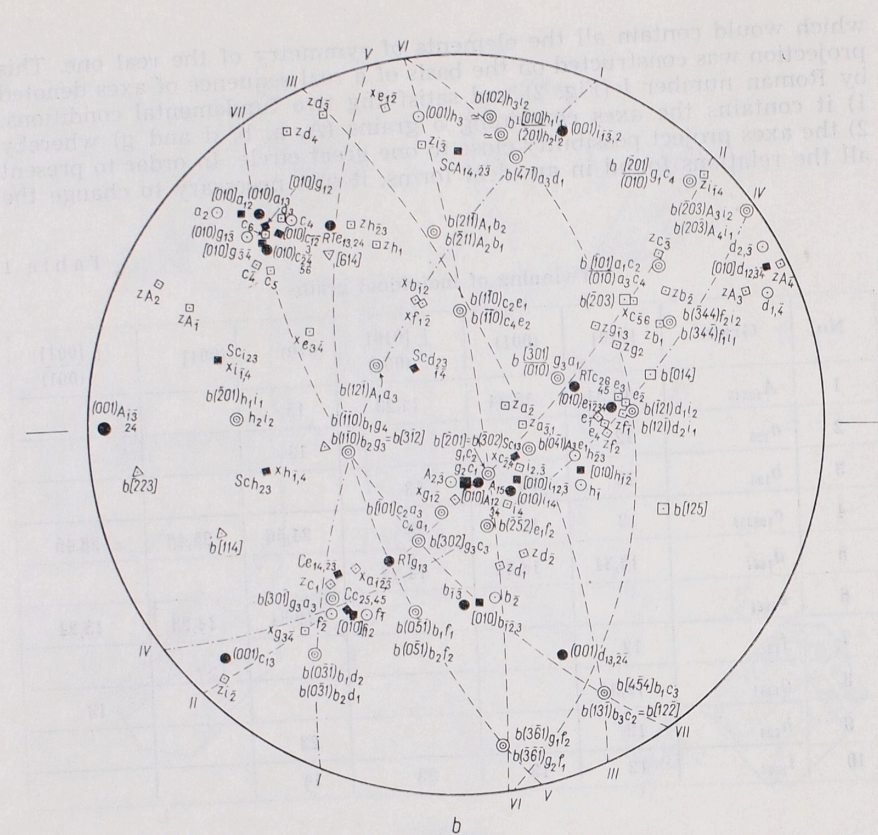


Fig. 2. Stereographic projection of oriented assemblage of grains presented in Fig. 1

- $$\left. \begin{array}{l} 1) b(31\bar{1}) - b_2 A_1 \\ 2) b(12\bar{1}) - A_1 a_3 \\ 3) b(50\bar{1}) - a_3 g_3 \\ 4) b(\bar{3}\bar{4}1) - g_3 b_2 \end{array} \right\} \not\propto = 46.5$$

As follows from Euler's law, the angles between the first and second as well as the third and fourth diads are equal. The axes 1 and 3, as well as 2 and 4 form couples of independent axes, i.e., have no common sub-individuals. The axes of the first couple are combined by means of the third one, the operation of which determines the origin of the fourth one (secondary).

On the real projection and, more abundantly, on the ideal one, "twin" axes belong to more than one sequence. Consequently, there result further transformations of some grains into others. It is easy to find that all the grains belong to one transformation cycle.

Similarly as in glomerophytic plagioclase intergrowths (grouping) (Gumowska-Wdowiak, 1974), we observe here individual sequences of

"twin" axes forming systems which simulate higher symmetry. Complete systems are formed triadic twin relations (Gumowska-Wdowiak 1974), whilst incomplete ones or their fragments result from simple twins. When the angles between four cooperating axes are equal or close to  $30^\circ$ ,  $45^\circ$ ,  $60^\circ$  or  $90^\circ$ , incomplete systems are formed displaying trigonal, tetragonal, hexagonal or orthorhombic pseudosymmetry. If this condition is satisfied by two angles only — the resulted sequence can be considered as a pseudosymmetric fragment.

From this point of view, the axial sequences can be characterised as follows:

Sequence I — 6 "twin" axes form two pseudotetragonal fragments ( $a$ ,  $b$ ) mutually connected by means of two common axes. The first of them is formed of grains  $A$ ,  $a$ ,  $b$  and  $g$ , whereas the second one of  $c$ ,  $b$ ,  $d$  and  $g$ . In the first case the pair of axes  $b[12\bar{1}]_{A_1a_3}$  —  $b(3\bar{4}1)_{b_2g_3}$  is connected with the second pair  $b(3\bar{1}1)_{A_1b_2}$  —  $b(50\bar{1})_{g_3a_3}$ . In the second one — this relation takes place between pairs  $\frac{b\perp[125]}{(501)} d_1b_2$  —  $b(50\bar{1})_{c_3g_3}$  and  $b(\bar{3}41)_{a_3d_1}$  —  $b(\bar{3}41)_{g_3b_2}$ . These both relations can be described by means of conventional symbols:

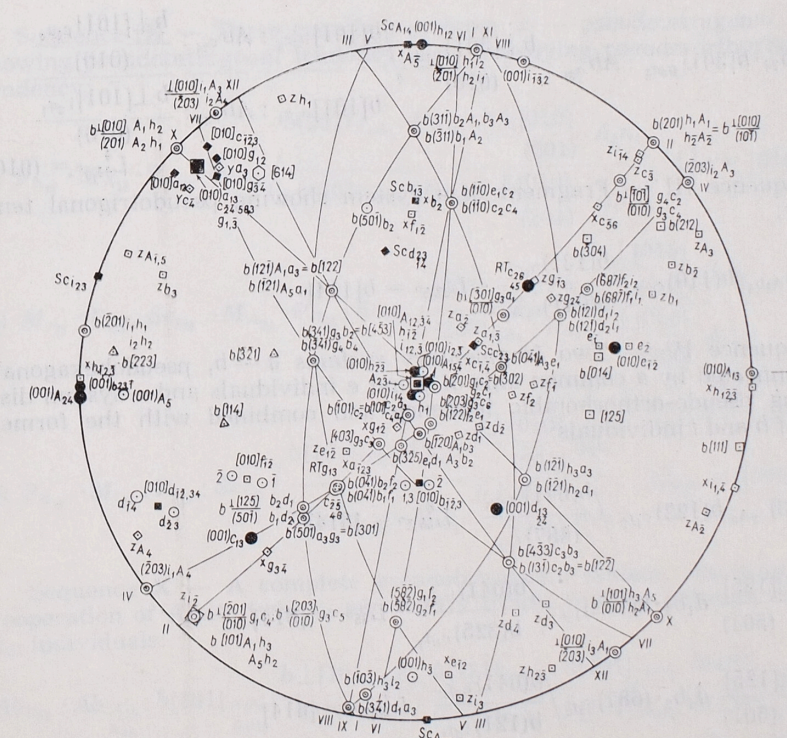


Fig. 3. Ideal stereographic projection of oriented assemblage of grains presented in Fig. 1

$$a) b(12\bar{1})_{a_5 A_1} \cdot b(\bar{3}\bar{4}\bar{1})_{b_2 c_3} / \frac{b(3\bar{1}\bar{1})_{A_1 b_2}}{b(501)_{g_3 a_3}} L_{46,5^\circ}^4 = [125]$$

$$b) b(50\bar{1})_{g_3 a_3} \cdot b \frac{\perp [125]}{(501)} / \frac{b(\bar{3}\bar{4}\bar{1})_{a_5 d_1}}{b(3\bar{4}\bar{1})_{g_3 b_2}} L_{43,5^\circ}^4 = [125]$$

The sequence of indices denotes the sequence of transformations. Sequence II — 2 complete pseudotetragonal systems, of which this denoted by  $a$  was formed by cooperation of Roc Tourné axis of the  $g$  grain and the twin triad Albite : Carlsbad : Roc Tourné of the  $c$  grain. Consequently, two new triads were formed:

$$a) RT_{31} \cdot C_{25} : Ab_{24} : RT_{26} / \frac{b[\bar{2}01]_{g_1 c_2} : (010)_{c_{24}} : \frac{b \perp [\bar{2}01]_{c_4 g_1}}{(010)}}{b[203]_{g_5 c_6} : (010)_{c_{65}} : \frac{b \perp [\bar{2}03]_{c_5 g_3}}{(010)}} L_{44,5^\circ}^4 = (010)$$

b) resulting from combination of Albite law of  $c_{24}$  grain with twin triad of the type  $[301] : Ab : \frac{\perp [301]}{(010)}$  of  $a$  and  $g$  grains:

$$b) Ab_{24} \cdot b[\bar{3}01]_{g_3 a_2} : Ab_{a_{31}} : \frac{b \perp [\bar{3}01]_{a_5 g_3}}{(010)} / \frac{b[\bar{1}01]_{a_5 c_2} : Ab_{c_{24}} : \frac{b \perp [\bar{1}01]_{c_4 a_8}}{(010)}}{b[\bar{1}01]_{a_1 c_4} : Ab_{c_{42}} : \frac{b \perp [\bar{1}01]_{c_2 a_1}}{(010)}} L_{44,5^\circ}^4 = (010)$$

Sequence III — Fragment of a system showing pseudotrigonal tendency:

$$b(3\bar{1}\bar{1})_{A_5 b_3} \cdot b(\bar{1}\bar{1}0)_{c_2 e_1} / \frac{b(13\bar{1})_{b_3 c_2}}{b(0\bar{4}1)_{e_1 A_3}} L_{52,5^\circ}^3 = b[114]$$

Sequence IV — Two fragmentary systems  $a - b$ , pseudohexagonal, are connected by a common axis of  $f$  and  $e$  individuals and  $c$  system displaying pseudo-orthorhombic tendency and combined with the former axes of  $b$  and  $i$  individuals:

$$a) (\bar{2}03)_{i_2 A_3} b(\bar{1}\bar{2}2)_{c_1 f_2} / \frac{b(0\bar{4}1)_{A_3 e_1}}{(687)_{f_2 i_2}} L_{30,5^\circ}^6 = [614]$$

$$b) \frac{b \perp [125]}{(501)} d_1 b_2 \cdot b(\bar{1}\bar{2}2)_{f_2 e_1} / \frac{b(0\bar{4}1)_{b_2 f_2}}{b(325)_{e_1 d_1}} L_{35^\circ}^6 = [614]$$

$$c) \frac{b \perp [125]}{(501)} d_1 b_2 \cdot (\bar{6}87)_{f_2 i_2} / \frac{b(0\bar{4}1)_{b_2 f_2}}{b(\bar{1}21)_{i_2 d_1}} L_{80,5^\circ}^2 = [614]$$

Sequence V — Fragment of a system showing pseudotetragonal tendency:

$$RT_{g_{13}} \cdot b(0\bar{4}1)_{b_2 f_2} / \frac{b(3\bar{4}1)_{g_5 b_2}}{b(582)_{f_2 g_1}} L_{39^\circ}^4 = b[041]$$

Sequence VI — Fragment of a system showing pseudotrigonal tendency:

$$b(\bar{3}02)_{g_1 c_2} \cdot b(\bar{1}\bar{2}2)_{e_1 f_2} / \frac{b(\bar{1}\bar{1}0)_{e_2 c_1}}{b(582)_{f_2 g_1}} L_{57^\circ}^3 = b[223]$$

Sequence VII — Fragment of a system showing intermediate tendency between tetragonal and hexagonal pseudosymmetry:

$$P_{b_{12}} \cdot b[403]_{g_3 c_3} / \frac{b[4\bar{5}3]_{b_2 g_3}}{b[4\bar{3}3]_{c_3 b_1}} L_{52^\circ}^{4-6} = b(\bar{3}04)$$

Sequence VIII — Fragment of a system displaying pseudotrigonal tendency:

$$b(3\bar{4}1)_{d_1 a_3} \cdot b(\bar{1}03)_{h_5 i_1} / \frac{b(\bar{1}\bar{2}1)_{a_3 h_3}}{b(121)_{t_2 d_1}} L_{64^\circ}^3 = b[\bar{3}21]$$

Sequence IX — Three complete systems:  $a$  — pseudotetragonal,  $b$  — showing pseudotetragonal tendency,  $c$  — displaying pseudo-orthorhombic tendency:

$$a) P_{h_{12}} \cdot M_{A_{13}} \cdot P_{A_{12}} : Sc_{A_{23}} / \frac{b(201)_{h_1 A_1} : P_{A_{12}} : \frac{b \perp [010]}{(201)}}{b(\bar{2}0\bar{1})_{h_2 A_2} : P_{A_{12}} : \frac{\perp [010]}{(201)}} A_2 h_1 L_{44^\circ}^4 = [010]$$

$$b) M_{i_{31}} : P_{i_{23}} : Sc_{i_{23}} \cdot M_{A_{24}} : P_{A_{43}} : Sc_{A_{32}} / \frac{(\bar{2}03)_{i_2 A_3} : P_{A_{31}} : \frac{\perp [010]}{(203)}}{(\bar{2}03)_{i_1 A_4} : P_{h_1 i_2} : \frac{\perp [010]}{(203)}} A_3 i_1 L_{55^\circ}^4 = [010]$$

$$c) P_{h_{12}} \cdot M_{i_{31}} : P_{i_{12}} : Sc_{i_{23}} / \frac{b(\bar{2}01)_{i_1 h_1} : P_{h_{12}} : \frac{b \perp [010]}{(201)}}{b(20\bar{1})_{i_2 h_2} : P_{h_{21}} : \frac{b \perp [010]}{(201)}} h_2 i_1 L_{80,50}^2 = [010]$$

Sequence X — A complete pseudotetragonal system, resulting from cooperation of Albite twin  $a_{13}$  and nearly triadic relation between  $A_{15}$  and  $h_{23}$  individuals:

$$Ab_{a_{31}} \cdot Ab_{A_{15}} : b[101]_{h_{23} A_5 h_2} / \frac{b \perp [101]_{A_1 h_2}}{(010)_{A_5 h_3}} / \frac{b(12\bar{1})_{a_3 A_1} : b[\bar{1}01]_{A_1 h_3} \cdot b(\bar{1}\bar{2}1)_{h_3 a_3}}{b(\bar{1}21)_{a_1 A_5} : b[101]_{A_5 h_2} \cdot b(\bar{1}21)_{h_2 a_1}} L_{43^\circ}^4 = b[101]$$

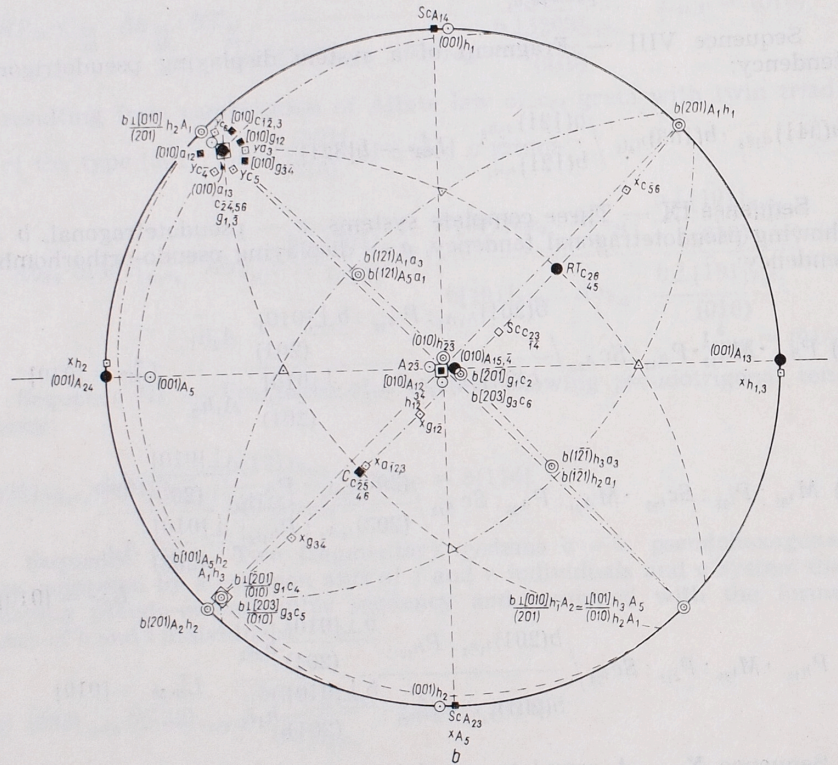
Sequence XI — A system displaying pseudo-orthorhombic tendency:

$$b(\bar{1}01)_{c_2d_3} \cdot b(\bar{3}\bar{2}\bar{5})_{d_1e_1} / \frac{b(3\bar{4}1)_{a_3d_1}}{b(\bar{1}10)_{e_1c_2}} L_{78^\circ}^2 = b[111]$$

Sequence XII — A fragment of pseudotetragonal system:

$$b[101]_{a_3c_2} \cdot b[\bar{1}20]_{A_1b_3} / \frac{b[12\bar{2}]_{a_3A_1}}{b[12\bar{2}]_{b_3c_2}} L_{47.5^\circ}^4 = b(212).$$

When analysing the mutual position of individual sequences of pseudo-symmetry, it is observed that they display a tendency toward cubic symmetry, it is formed due to pseudosymmetry. The first system presented in Fig. 4, was formed due to superposition of three pseudotetragonal ones (IIa, IXa — X), the tetrad to superposition of three pseudotetragonal ones (IIa, IXa — X), the tetrad to



axes of which are mutually nearly perpendicular. This system consists of 5 grains: A, a, c, g and h, while the second one of the grains a, g and b, supplemented by a possible individual j<sub>1</sub> and two albite subindividuials b<sub>1</sub> and d<sub>1</sub>. The latter is formed by cooperation of twin triad of pseudotetragonal sequence IIb and pseudotetragonal one Ib (Fig. 5). Pseudocubic system of this type results from cooperation of the triad:

$$b[\bar{3}01] : Ab : b \perp [30\bar{1}]_{(010)}, b[\bar{5}01] : [125] : b \perp [\bar{1}25]_{(\bar{5}01)} \text{ and } b(34\bar{1}) : b[125] : b \perp [125]_{(34\bar{1})}.$$

The first system can be considered as representing superior symmetry resulting from superposition of lower symmetric systems, whereas the second one originated from triadic transformations (Gumowska-Wdowiak, 1974).

The presence of only two pseudocubic systems combining 7 or 10 grains does not exclude the existence of other ones if we will take into

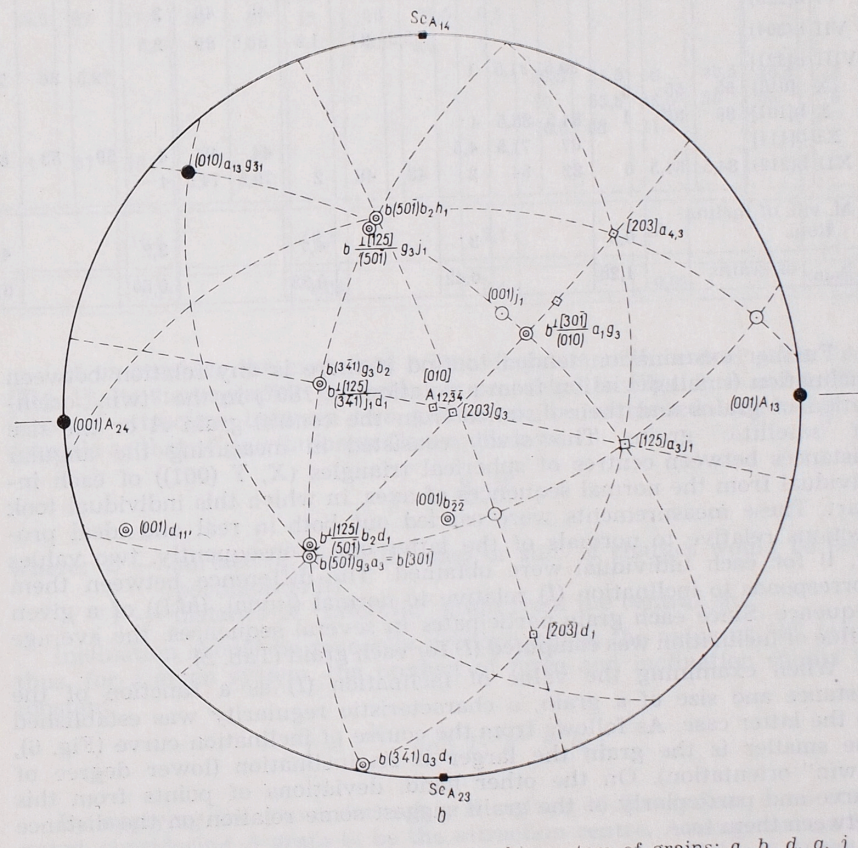


Table 2

## Inclination of "twin"

Nr seq- uen- ce	Grain [uvw] (hkl)	A			a			b			c			d		
		r	i	I	r	i	I	r	i	I	r	i	I	r	i	I
I	b[125]	76	75	1	81,5	77	4,5	37,5	37	0,5	53	52,5	0,5	28,5	26	2,5
II	(010)				57	58,5	1,5									
III	[614]	23,5	24	0,5				80	89	9	26,5	31,5	5			
IV	b[114]	45,5	45,5	0				89	83	6				88	89,5	1,5
V	b[014]							29,5	21,5	3						
VI	b[223]										45	48	3			
VII	b(304)							35,5	34	1,5	86,5	89	2,5			
VIII	b[321]				30,5	31,5	1							79,5	86	7,5
IX	[010]	55	55	0												
X	b[101]	89	88	1	84,5	88,5	4									
XI	b[111]				67	71,5	4,5				44	48	4	59	53	6
XII	b(212)	84,5	84,5	0	82	84	2	48	46	2	70,5	74,5	4			
M. val. of inclina- tions		0,5			3			4,7			3,2			4,4		
S <sub>mm<sup>2</sup></sub> of grains		1,28			0,42			0,33			0,60			0,58		

Further examination tended to find if there is any relation between inclination (small deviation from a rotation by 180°) in the "twin" orientation of grains and their distance from the central grain A or the size of "satellitic" grains. This study consisted in measuring the angular distances between centres of spherical triangles (X, Y (001)) of each individual from the normal sequences of axes, in which this individual took part. These measurements were carried out both in real and ideal projections relative to normals of the latter one. Consequently, two values (*r*, *i*) for each individual were obtained. The difference between them corresponds to inclination (*I*) relative to normal ([uvw], (hkl)) of a given sequence. Since each grain participates in several sequences, the average value of inclination was computed (*I*) for each grain (Tab. 2).

When examining the value of inclination (*I*) as a function of the distance and size of a grain, a characteristic regularity was established in the latter case. As follows from the course of inclination curve (Fig. 6), the smaller is the grain the larger is its inclination (lower degree of "twin" orientation). On the other hand, deviations of points from this curve and particularly of the grain suggest some relation on the distance between them too.

If long range forces acting in magmatic melt are responsible for the formation of glomerophytic intergrowths of phenocrysts — synneusis aggregates (Vance 1969), the values of inclination, grain sizes and the distances of grains from the central one should be concordant with mathematical presentation of these forces. On the other side, such concordance would indicate the possibility of existence of the forces in question.

## orientation of grains

e			f			g			h			i			
<i>r</i>	<i>i</i>	<i>I</i>													
						88	88	0							
						57	58	1							
66,5	81,5	15													
35,5	48,5	13	73,5	89,5	16										
			43	22	21	89	89	2							
69,5	87	17,5	59	47	12	80	79,5	0,5							
						83	90	7							
									37,5	31,5	6	40,5	38,5	2	
									37	55,5	18,5	50	55	5	
									76,5	88	11,5				
71	87	16													
						16,4			16,2			2,1		12	
															5
						0,11			0,08			0,4		0,07	1,98

Let us consider the examined oriented system with central grain "A" (Fig. 1). Its stereographic projection is presented in Figs. 2, 3 and 4. The force of attraction between two grains can be expressed by analogical formula as that of gravitation or Coulomb's law:

$$F' = \frac{S_1 \cdot S_2}{r^2}$$

where: *S* — surface of grain (its mass or sum of charges would be proportional to it),

*r* — distance of "satellitic" grain from the central one.

Inclination should be inversely proportional to the value of "F" force. thus, for a given system, the product of force and inclination should be constant:

$$I = \frac{K}{F'} \text{ and } I \cdot F' = K$$

By applying the above formulas, *K* values of the system were computed, considering *A* grain to be the attraction centre. Average means for inclinations of central and satellitic grains are given in Table 2. Though the surface of grains (*S*) but approximately determines their sizes, very good concordance of *K*<sub>1</sub> value was obtained. For all the grains, except "g" and "h", the *K*<sub>1</sub> value vary within the limits 1.26—1.62 (Tab. 3). Since *K*<sub>3</sub> values for "g" and "h" grains are nearly the same (0.22 and 0.25) and because these grains are situated closer to large grain "i" (Fig. 1), and because these grains are situated closer to large grain "i" (Fig. 1), further calculations for a system with the latter grain as the central one

were carried out (Tab. 3 — second part). In this case the constant for „g” and „h” grains as well as that for similarly distant „a” grain was close to  $K_1$ . The constants for remaining grains were very close, ranging from 0.51 to 0.59 ( $K_2$ ). Relationship between inclination “ $I$ ” and the force “ $F$ ” is presented in Fig. 7. In this diagram, projection points are distributed along hyperbolic curves indicating average values of  $K_1$ ,  $K_2$  and  $K_3$  (1.38, 0.535 and 0.235). It should be noted that the ratio of these values is approximately 1 : 0.4 : 0.16, so that each successive value is 2.5 times smaller than the preceding one. Calculation of constants for any arbitrary combination of grains have given diversified results. Consequently, only  $A$  and “ $i$ ” grains can be considered as attraction centres. Oriented systems

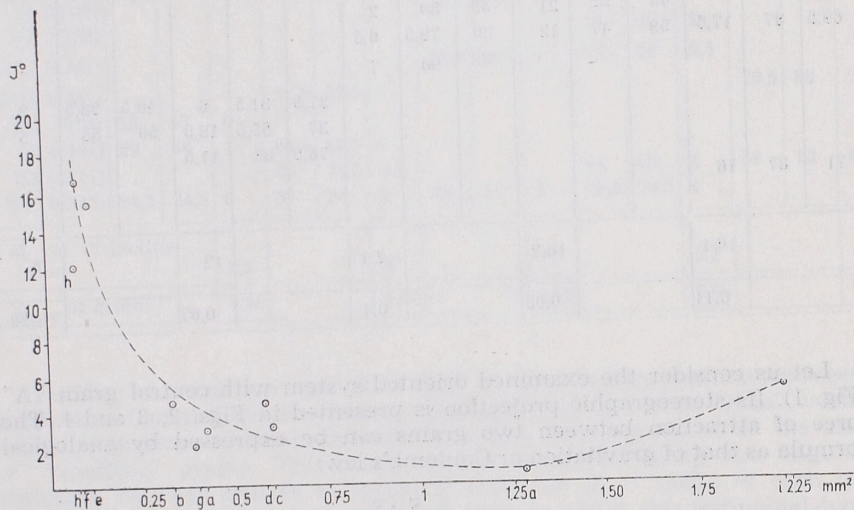


Fig. 6. Diagram showing relation between “twin” orientation of grains and their size

of grains (synneusis assemblages \*) represent, unquestionably, an intermediate stage of development of glomerophytic intergrowths (synneusis aggregates). Fairly constant values of  $K$  indicate that these both forms are due to the activity of long range forces in magmatic melt. Three numerical values of  $K$  computed are, most probably, due to complexity of this process being the result of interaction of several attraction centres. This conclusion is confirmed by the structure of the rock in question where numerous orbital systems are observed. Consequently, each grain belongs to more than one of these systems. It is supposed that interaction of several attraction centres could result in establishing a state of energetic equilibrium; processes of crystal aggregation are inhibited. Lack of glomerophytes consisting of larger amounts of grains differs the rock in question from other varieties of andesites of the Pieniny series (Gumowska-Wdowiak, 1974). Simultaneously, this phenomenon can be considered as an argument for correctness of the above hypothesis. It is supposed that

this type of porphyric textures is connected with peculiar mechanical conditions of consolidation, when no violent turbulences or any other intense lava movements took place.

Detailed quantitative analysis of oriented systems of grains clearly indicates the activity of long range forces in magmatic melt. In this

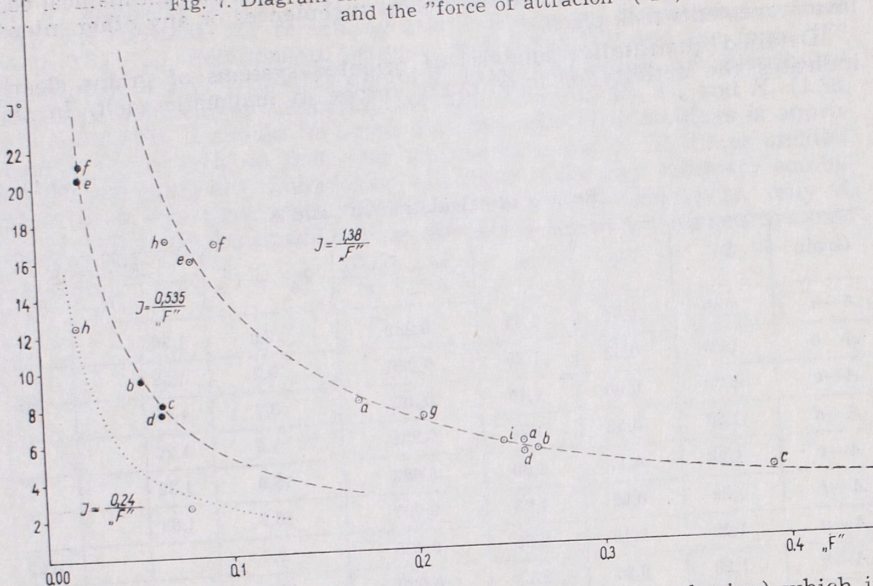
Table 3  
Results of calculation „ $F$ ” and  $K$

Grain	$S_A$	$S_X$	$r$	$\frac{S_A S_X}{r^2}$	$I'_A + I'_X$	$\frac{F}{r} \cdot I = K$		
						$K_1$	$K_2$	$K_3$
$A-a$	1,28	0,42	1,44	0,259	5,0	1,30		
$A-b$	1,28	0,33	1,26	0,266	5,2	1,38		
$A-c$	1,28	0,60	1,40	0,392	3,7	1,45		
$A-d$	1,28	0,58	1,70	0,258	4,9	1,26		
$A-e$	1,28	0,11	1,30	0,083	15,9	1,32		
$A-f$	1,28	0,08	1,03	0,097	16,7	1,62		
$A-g$	1,28	0,40	2,55	0,085	2,6			0,22
$A-h$	1,28	0,07	2,11	0,020	12,5			0,25
	$S_i$	$S_X$	$r$	$\frac{S_i S_X}{r^2}$	$I'_A + I'_X$			
$i-A$	1,98	1,28	2,93	0,248	5,5	1,36		
$i-h$	1,98	0,07	1,40	0,071	17	1,21		
$i-g$	1,98	0,40	1,96	0,206	7,1	1,46		
$i-a$	1,98	0,42	2,21	0,171	8	1,37		
$i-b$	1,98	0,33	3,46	0,055	9,7		0,53	
$i-c$	1,98	0,60	4,24	0,065	8,2		0,53	
$i-d$	1,98	0,58	4,26	0,063	9,4		0,59	
$i-e$	1,98	0,11	2,87	0,025	20,4		0,51	
$i-f$	1,98	0,08	2,46	0,026	21,2		0,55	

concrete case it was possible to catch this activity in the very act whilst in glomerophytic intergrowths we can observe merely their effects. Though all the regularities established are evidently documenting the existence of the forces in question, their nature is still problematic. If these forces are responsible both for attraction of crystals and their preferred orientation (resulting from their “twin” orientation in rock matrix), we may suggest that these forces are electrostatic in nature. Preferred orientation and mutual attraction of grains can be due to electric polarity of crystals suspended in the melt. Distribution of electric charges resulting in dipole moments of these particles can be responsible for drifting together and union of phenocrysts. The activity of long range forces does not

\* The term proposed in accordance with Vance's nomenclature (1969).

Fig. 7. Diagram showing relation between inclination ( $I'$ ) of grains and the "force of attraction" ("F")



exclude the influence of the short range ones (e.g. of cohesion) which in the phenomenon under consideration play an auxiliary role.

Acknowledgments: The author is deeply indebted to Prof. Antoni Łaszkiewicz for valuable discussions and critical remarks.

#### REFERENCES

- GUMOWSKA-WDOWIAK Z., 1974: Twin intergrowths of plagioclase in glomerophytic andesites of the Pieniny Mts. in Poland. *Miner polon.* 5.  
VANCE J. A., 1969: Synnousis. *Contr. Miner. Petr.* 24, no 1. Berlin — Heidelberg — New York.

Zofia GUMOWSKA-WDOWIAK

#### ORIENTOWANE ZESPOŁY FENOKRYSTAŁÓW PLAGIOKLAZÓW W ANDEZYTACH OKOLIC PIENIN

#### Streszczenie

Przedmiotem badań są zespoły zbliżniaczych (tab. 1) fenokryształów plagioklazu w andezytach okolic Pienin (fig. 1). Poszczególne ziarna — podobnie jak w zrostach — znajdują się względem siebie w położeniami bliźniaczymi (fig. 2). Osie bliźniacze tworzą ciągi wzajemnych zależności geometrycznych (I—VIII, fig. 2), chociaż nie układają się dokładnie na wspólnych kołach wielkich. Spowodowane to jest przede wszystkim niewielkimi odchyleniami (inklinacją) od obrotu o  $180^\circ$ . Stąd wnikliwsze ba-

dania należało przeprowadzić na rzucie idealnym; jako konsekwencje tego rzutu powstały dalsze 4 ciągi od IX do XII (fig. 3). Podobnie jak w zrostach glomerofirowych plagioklazu (Gumowska-Wdowiak 1974), tak i tu poszczególne ciągi tworzą układy (lub fragmenty) o wyższej pseudosymetrii od rombowej do heksagonalnej. Co więcej, w wyniku wzajemnego ich współdziałania utworzyły się dwa układy o tendencji pseudoregularnej (fig. 4, 5), z których drugi uzupełniony został możliwym osobnikiem  $j_1$  i subindywidualnymi albitowymi  $b_1'$  i  $d_1'$ . Badając wartości inklinacji (tab. 2,  $I$  — uśrednione wartości inklinacji ziarn wyliczone jako różnice odległości kątowych środków trójkątów sferycznych biegunów X, Y i (001) od normalnych ciągów na rzucie idealnym i rzeczywistym) jako funkcję wielkości ziarn stwierdzono, że im większe ziarno, tym mniejsza inklinacja, tzn. tym większy stopień orientacji „bliźniaczej” (fig. 6).

Praca zawiera dalsze rozważania na temat możliwości działania w stopie magmowym sił dalekiego zasięgu, odpowiedzialnych za proces tworzenia się zrostów glomerofirowych, których stadium pośrednie stanowią zespoły orientowane (układy orbitalne). Zależności matematyczne, które wystąpiły między wielkością ziarn (powierzchnia  $S$ ), ich odległością ( $r$ ) względem ziarna centralnego ( $A$  i „ $i$ ”) i inklinacją ( $I$ ), według wprowadzo-

nnych wzorów: „ $F$ ” =  $\frac{S_1 S_2}{r^2}$  (analogiczny do prawa grawitacji lub Coulomb'a), i „ $F$ ” =  $K$  (const.) dowodzą istnienia tych sił (tab. 3, fig. 7). Pojawienie się trzech serii  $K$  ( $K_1$ ,  $K_2$ ,  $K_3$ ) wskazuje na wzajemne oddziaływanie większej liczby ośrodków przyciągających (w badanym układzie ziarna  $A$  i „ $i$ ”). W wyniku takiego oddziaływania może powstać pewien stan równowagi energetycznej w stopie, hamujący dalszy proces łączenia się kryształów. Obraz mikroskopowy skały potwierdza ten wniosek. Zjawisko łączenia się i wzajemnego orientowania się ziarn najłatwiej tłumaczy się działaniem sił elektrostatycznych.

#### OBJASNIENIA DO FIGUR

- Fig. 1. Orientowane zespoły ziarn plagioklazu w andezycie z potoku Krupianka, Pieniny  
Fig. 2. Projekcja stereograficzna orientowanych zespołów ziarn przedstawionych na fig. 1  
Fig. 3. Wyidealizowana projekcja stereograficzna orientowanych zespołów ziarn przedstawionych na fig. 1  
Fig. 4. Projekcja stereograficzna pseudo-regularnego zespołu ziarn:  $A$ ,  $a$ ,  $c$ ,  $g$ ,  $h$   
Fig. 5. Projekcja stereograficzna pseudo-regularnego zespołu ziarn:  $a$ ,  $b$ ,  $d$ ,  $g$ ,  $j$   
Fig. 6. Diagram wykazujący zależność pomiędzy orientacją bliźniaczą ziarn a ich wielkością  
Fig. 7. Wykres inklinacji ziarn jako funkcji „ $F$ ”

Зофия ГУМОВСКА-ВДОВИАК

ОРИЕНТИРОВАННЫЕ КОМПЛЕКСЫ ФЕНОКРИСТАЛЛОВ  
ПЛАГИОКЛАЗОВ В АНДЕЗИТАХ РАЙОНА ПЕНИН

Резюме

Предметом анализа были комплексы двойниковых фенокристаллов плагиоклазов в андезитах района Пенин (фиг. 1). Отдельные зерна располагаются относительно друг друга в двойниковых позициях (фиг. 2). Двойниковые оси образуют последовательные геометрические связи (I — VIII, фиг. 2), хотя и не располагаются на общих окружностях. Это обусловлено, прежде всего, небольшими отклонениями (инклинацией) от поворота на  $180^\circ$ . В связи с этим более детальные наблюдения следовало провести на идеальной проекции. Последствием этой проекции были дальнейшие связи IX — XII (фиг. 3). Подобно гломерофировым срастаниям плагиоклазов (Гумовска-Вдовиак 1974) так и здесь отдельные связи образуют системы псевдосимметри высшего порядка — от ромбической по гексагональную. Более того, в итоге их взаимодействия образовались две системы с псевдокубическими признаками (фиг. 4, 5), вторая из которых дополняется возможным индивидом  $j_1$  и субиндивидами альбита  $b'_1$  и  $d'_1$ . Путем определения величины инклинации (таб. 2, I — средние значения инклинации зерен), представляющей разницу угловых расстояний середин треугольников сферических полюсов X, Y и (001) от нормалей двойниковых связей в идеальной и истинной проекциях, что обусловлено величиной зерен, было констатировано, что чем больше зерно, тем меньшая инклинация, т. е. тем высшая степень „двойниковой“ ориентировки (фиг. 6).

В работе также рассматривается возможность сил дальнего действия в жидкой магме, содействующих образованию гломерофировых сростков, промежуточной стадии которого являются ориентированные скопления (орбитальные системы). Математические зависимости между величиной зерна (поверхность разреза —  $s$ ), расстояние ( $r$ ) от центрального зерна ( $A$ , „ $i$ “) и инклинации ( $I$ ) по формуле: „ $F$ “ =  $\frac{S_1 S_2}{r^2}$  (аналогично Ньютона, Кулемба и „ $F$ “ ·  $I$  =  $K$  (константа). Величины константы  $K$  вычисленные (Таб. 3, фиг. 7) указывают что действительно существуют силы дальнего действия. Получение трех серий  $K$  ( $K_1$ ,  $K_2$ ,  $K_3$ ) указывает на действие ряда центров взаимодействия в ориентированных скоплениях. Результатом взаимодействия появляется определенное энергетическое равновесие, тормозящее дальний процесс соединения отдельных зерен в гломерфиры. Микроскопическая картина подтверждает это заключение. Соединение зерен и их взаимная ориентировка легче всего объясняется действием электростатических сил.

ОБЪЯСНЕНИЯ К ФИГУРАМ

- Фиг. 1. Ориентированные комплексы зерен плагиоклазов в андезите ручья Крупянка в Пенинах  
Фиг. 2. Стереографическая проекция ориентированных комплексов зерен, представленных на фиг. 1

Фиг. 3. Идеализированная стереографическая проекция ориентированных комплексов зерен, представленных на фиг. 1

Фиг. 4. Стереографическая проекция псевдокубического комплекса зерен:  $A$ ,  $a$ ,  $c$ ,  $g$ ,  $h$

Фиг. 5. Стереографическая проекция псевдокубического комплекса зерен:  $a$ ,  $b$ ,  $d$ ,  $g$ ,  $j$

Фиг. 6. Диаграмма, изображающая зависимость между двойниковой ориентировкой зерен и их величиной